The effects of aortic coarctation on cerebral hemodynamics and its importance in the etiopathogenesis of intracranial aneurysms

----

Singh, Pankaj K; Marzo, Alberto; Staicu, Cristina; William, Matt G; Wilkinson, Iain; Lawford, Patricia V; Ruefenacht, Daniel André; Bijlenga, Philippe Alexandre Pierre; Frangi, Alejandro F; Hose, Rodney; Patel, Umang J; Coley, Stuart C

The Effects of Aortic Coarctation on Cerebral Hemodynamics and its Importance in the Etiopathogenesis of Intracranial Aneurysms

Abstract

Pankaj K Singh, MRCS
Alberto Marzo, PhD
Cristina Staicu, PhD
Matt G William, PhD
Iain Wilkinson, PhD
Patricia V Lawford, PhD
Daniel A Rufenacht, MD
Philippe Bijlenga, MD
Alejandro F Frangi, PhD
Rodney Hose, PhD
Umang J Patel, FRCS
Stuart C Coley, MD

Address Correspondence to:
Pankaj K Singh, MRCS
Clinical Research Fellow,
Departments of Neurosurgery/Medical Physics,
Royal Hallamshire Hospital, Sheffield, UK
Email: neurosurgery2007@gmail.com
Ph: +44 114 2712180
Fax: +44 114 2713314

Objectives: Hemodynamic changes in the cerebral circulation in presence of coarctation of aorta (CoA) and their significance in the increased intracranial aneurysms (IAs) formation in these patients remain unclear. In the present study, we measured the flow-rate waveforms in the cerebral arteries of a patient with CoA, followed by an analysis of different hemodynamic indices in a coexisting IA.

Materials and Methods: Phase-contrast Magnetic Resonance (pc-MR) volumetric flow-rate (VFR) measurements were performed in cerebral arteries of a 51 years old woman with coexisting CoA, and five healthy volunteers. Numerical predictions of a number of relevant hemodynamic indices were performed in an IA located in sub-clinoid part of left internal carotid artery (ICA) of the patient. Computations were performed using Ansys®-CFX™ solver using the VFR values measured in the patient as boundary conditions (BCs). A second analysis was performed using the average VFR values measured in healthy volunteers. The VFR waveforms measured in the patient and healthy volunteers were compared followed by a comparison of the hemodynamic indices obtained using both approaches. The results are discussed in the background of relevant literature.

Results: Mean flow-rates were increased by 27.1% to 54.9% (2.66-5.44 ml/sec) in the cerebral circulation of patients with CoA as compared to healthy volunteers (1.2-3.95 ml/sec). Velocities were increased inside the IA by 35-45%. An exponential rise of 650% was observed in the area affected by high wall shear stress (WSS>15Pa) when flow-rates specific to CoA were used as compared to population average flow-rates. Absolute values of space and time averaged WSS were increased by 65%. Whereas values of maximum pressure on the IA wall were increased by 15% the area of elevated pressure was actually decreased by 50%, reflecting a more focalized jet impingement within the IA of the CoA patient.

Conclusions: IAs can develop in patients with CoA several years after the surgical repair. Cerebral flow-rates in CoA patients are significantly higher as compared to average flow-rates in healthy population. The increased supra-physiological WSS (>15Pa), OSI (>0.2) and focalized pressure may play an important role in the etiopathogenesis of IAs in patients with CoA.

Keywords: Coarctation of aorta, intracranial aneurysms, cerebral circulation, flow-rates, hemodynamics, wall shear stress, computational fluid dynamics

Introduction:

Estimated annual incidence of IAs in most Western countries is estimated to be at 1 to 2%.[7,49] Subarachnoid hemorrhage (SAH) can be a consequence with a high overall mortality rates approximating 45% (range 32-67%).[46] About 30% of survivors have moderate to severe disabilities and 66% of those who have 'successful' clip placement, never return to same quality of life as before SAH.[23,46] The current evidence convincingly supports a multi-factorial basis for the initiation and rupture of IAs.[88,92,108]

Amongst other etiologies proposed, CoA has been highlighted as a major risk factor in the etiopathogenesis of IAs.[1,3,15,24,27,48,50,53,62,70,75,78,87] A wide range for the incidence of IAs in patients with CoA has been reported starting from 2.5%[1] to as high as 50%,[89] all above the estimated

incidence of IAs in general population. Connolly and colleagues in their recent study confirmed that the frequency of IAs among patients with CoA is approximately 5 times higher than that of the general population.[15] The incidence of IA rupture in CoA patients (4.8%)[70,83] is also higher than the estimated rate of rupture in the general population which is less than 1%.[106] In spite of CoA being a well-established risk factor for IA formation,[1,3,15,24,27,48,50,53,62,70,75,78,87] the exact underlying mechanisms for this association remain poorly understood. Hypertension[3,9,24,50,75,78,92,95] and developmental errors of neural crest resulting in abnormal vessel wall collagen[15,17,48,53,62,70,87], are two main factors thought to facilitate the formation of IAs in presence of CoA. It is surprising to note that in spite of well established role of wall shear stress (WSS) in the genesis of IAs,[11,32,38,40–42,65,69,72,91,104] none of the workers explored this important link in this context.

Owing to their direct origin from the pre-coarctation segment of aorta, cerebro-cephalic arteries are most likely to be affected by the hemodynamic changes occurring in this part of aorta. Secondary to the increased resistance to outflow, increased aorto-cranial pressure gradients have been demonstrated by a number of authors correlating to the severity of stenosis.[1,36,45,71,102] Dilatation of cervico-cephalic arteries in CoA secondary to this increased pressure gradient is has also been reported.[1,85]

An increase in the radius (r) of cerebral arteries and increased aorto-cranial pressure gradient (ΔP) in CoA are expected to result in an exponential rise in flow-rates (Q) as per the Hagan-Poiseuille law (Equation-1), given the viscosity (μ) and length (L) remain constant.

$$Q = \frac{\Delta P}{8 \mu L} \pi r^4 \quad \text{............ (Eq-1)}$$

Furthermore, bradycardia coupled with increased stroke volume

and cardiac output is a known feature of CoA.[36] These increments will further increase the cerebral blood-flow (CBF).

An increased flow-rate (Q), in turn is one of the major factors responsible for increased wall shear stress (WSS) in the intracranial arteries (Equation-2).

$$\tau = 4 \mu \frac{Q}{\pi r^3} \quad \text{............... (Eq-2)}$$

Where τ is WSS

Literature seems to be particularly deficient and controversial on the effects of CoA on cerebral arterial flow-rates. After a thorough search (PubMed®, Embase® and Google-Scholar™ searched from the year 1900 up to 2009) we could retrieve only two relevant studies. In 1949 Hafkenschiel et al[37] demonstrated a significant increase in cerebral arterial flow-rates in patients with CoA. Rowe and colleagues[85] found no significant differences in the flow-rates before and after the repair of CoA in their study done in 1964. No apparent efforts were done since then to measure the cerebral arterial flow-rates in patients with CoA. Paucity of information about the flow patterns inside the cerebral circulation in presence of CoA provided us a rationale to measure the cerebral arterial flow-rates in the present patient. Furthermore, given the widely accepted importance of hemodynamics in the etiopathogenesis of IAs[11,32,38,40–42,65,69,72,91,104] it is logical to analyze the hemodynamic factors in the coexisting IA of our patient. A better understanding of the etiopathogenesis of the IA formation and rupture may help clinicians in preventing and treating the disease effectively.

In the current study, we preformed pc-MR measurements in the cerebral arteries of a CoA patient with coexisting IA and five healthy volunteers followed by an analysis of the different hemodynamic factors inside IA. The possible role of
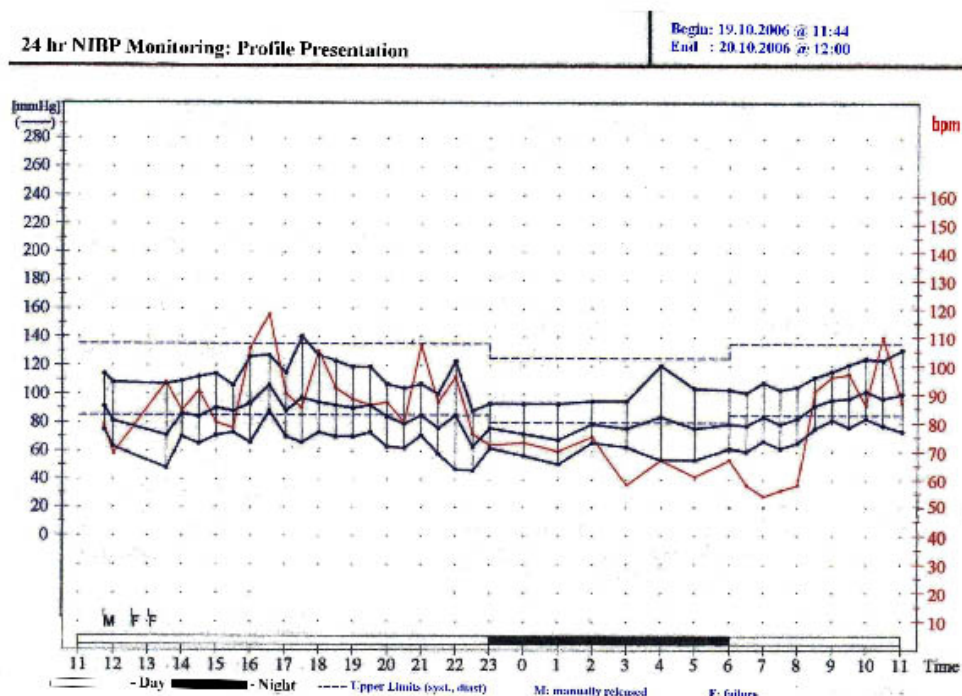

Figure 1: 24 hours ambulatory Non-invasive BP (NIBP) monitoring showing satisfactory BP control for both systolic and diastolic values.
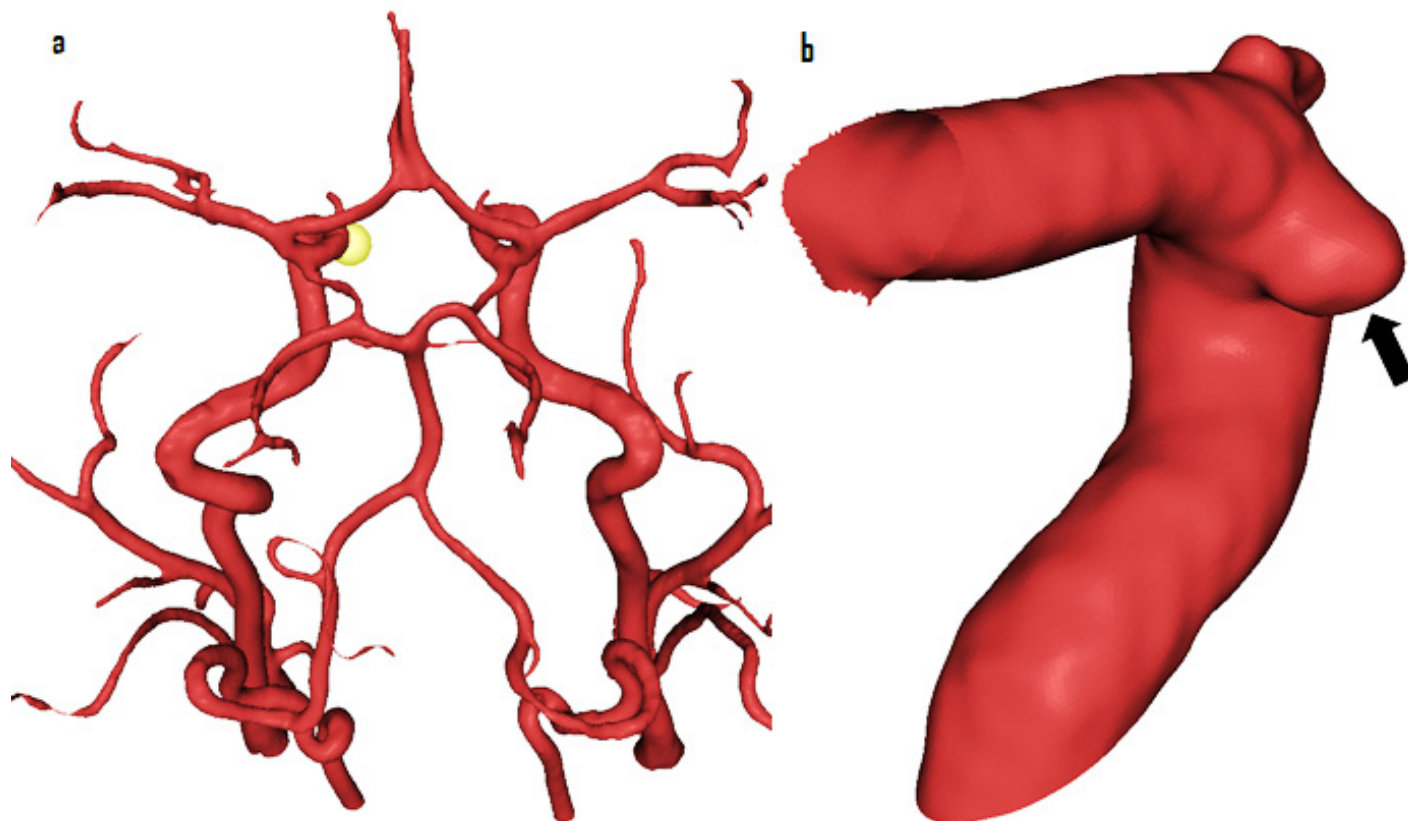
Figure 2: Intracranial aneurysm included in the study shown in (a) circle of Willis (yellow sphere- arrowhead) and (b) in subclinoid part of ICA (arrow)

hemodynamics is discussed in this context in a background of relevant literature.

Materials and methods

The study was conducted jointly in the departments of Neurosurgery and Neuroradiology, Royal Hallamshire Hospital, and the Academic Unit of Medical Physics, and Radiology, School of Medicine and Biomedical Sciences, University of Sheffield, Sheffield, UK. After obtaining appropriate consent and ethical approval the patient was recruited to the @neurIST project (www.aneurist.org).

Clinical details: This 51 years old woman, presented for the first time to cardiovascular surgeons in 1989 at the age of 31 years through obstetric unit. She had hypertension during both her pregnancies but was otherwise asymptomatic. She was a cigarette smoker, smoking 10-15 cigarettes per day. On clinical examination, she appeared fit and well with a blood pressure (BP) of 160/90 mm Hg. No femoral pulses were palpable and there was an ejection systolic murmur in the aortic area coupled with a continuous machinery murmur at left scapula. She was taking oral antihypertensives (Atenolol and Nifedipine) to control her hypertension. Subsequent investigations including DVI (digital vascular scan) done at that time revealed a severe (>80% reduction in diameter) post-ductal aortic coarctation distal to origin of left subclavian artery. X-ray chest showed typical inferior notching of 3rd and 8th ribs, bilaterally. No other congenital anomalies were detected apart from a pseudo-bicuspid aortic valve, without any

evidence of regurgitation or stenosis. One year later, the patient was treated with Dacron onlay patch graft (DOPG) repair for her coarctation with an uneventful postoperative recovery.

A follow-up MRI of heart done in July 2004 after 15 years of primary procedure demonstrated evidence of re-occurrence of coarctation with significant (60-70%) loss of luminal diameter. The stenosis occurred just distal to the origin of left subclavian artery coinciding with the site of repair. Presence of significant collaterals was also noted along with marginal concentric hypertrophy of left ventricle but adequate ejection fraction. A BRUCE treadmill stress test done to evaluate cardiac fitness demonstrated an appropriate exercise tolerance without any chest pain or ECG changes. A 24-hour BP monitoring further confirmed a satisfactory BP control (Fig-1). A completely asymptomatic status with no signs of cardiac failure was the reason to manage her conservatively.

The patient was referred to Neurosurgery in May 2007 with complaints of tingling and numbness affecting right side of her face. On further interrogation, she gave history of a similar episode three years back resulting in spontaneous resolution, but no other neurological symptoms. On clinical examination, she had no neurological deficits. An MRI demonstrated presence of two incidental IAs. First aneurysm was located in the pericallosal artery and was 4.2 mm in maximum diameter. A second small broad necked 1 mm aneurysm was also present at the origin of left anterior temporal artery arising from the proximal left middle cerebral artery (MCA). The findings were further confirmed by a

3D rotational angiogram (3DRA), which apart from two previous IAs, also revealed an approximately 1.8 mm aneurysm in the subclinoid segment of left internal carotid artery (ICA), pointing medially (Fig-2). The case was discussed in a multidisciplinary meeting with Neuroradiologists and it was found that due to its small neck the pericallosal IA was suitable for coil embolization.

3DRA acquisition: All medical images were obtained using rotational acquisition in a Philips® Integris™ Allura machine (Philips® Medical Systems, Best, The Netherlands), producing 100 images in 6 seconds, with 5 ms exposure per image. Voxel size in the reconstructed 3D images was 121 microns with reconstruction matrix of 512 x 512 x 512.

Endovascular Interventions: The pericallosal artery aneurysm was embolized under general anaesthesia in May 2008 with GDC® (Guglielmi Detachable Coils). A 6-french guided catheter was gently placed within the distal right internal carotid artery (ICA). The aneurysm was catheterized with an Excelsior® SL-10 microcatheter using a Transend® 14 guidewire (Boston Scientific, USA). The IA was packed satisfactorily using four Micrus® Cerecyte® endovascular bare platinum coils. She made an uneventful recovery from the procedure. Owing to their small size and anticipated difficulties for endovascular coiling (broad neck) remaining two aneurysms were decided to be observed by follow-up MRAs.

Flow Measurements & pc-MR protocol: MR imaging was performed at high field strength (Achieva™ 3.0T, Philips® Medical Systems, Best, The Netherlands) using a standard 8-channel, radiofrequency receive-only head coil. The same radiographer imaged the patient and all volunteers to maximize reproducibility of overall acquisition technique. Macroscopic vascular flow and IA location were visualized using a qualitative Time-Of-Flight (TOF) MR angiography sequence (TR=25 ms; TE=3.5 ms; α=20°; visualization voxel size = 0.39 x 0.39 x 1.00 mm³). Maximum intensity projections from this 3D dataset were used to define the placement of each quantitative phase contrast measurement plane perpendicular to the vessel under investigation. A 2D acquisition sequence (TR=8 ms; TE=4.4 ms; α=10°; field of view=220 x 179 mm;² in-plane acquisition matrix=128 x 112; slice thickness=5 mm) was used to acquire 40 velocity-encoded 'time points' over the cardiac cycle at each vascular location. Vector ECG triggering was used to standardize each quantitative acquisition.

The measurements were performed at three locations, both in healthy volunteers and in patient viz. left proximal ICA, left distal ICA, and left ACA A-1 segment. An appropriate maximum velocity-encoding (VENC) value was chosen (100 cm/sec) for ICA to ensure that appropriate dynamic ranges were sampled in all cases and no phase-aliasing occurred. As proximal vessels geometry has an important influence on intra-aneurysmal hemodynamics,[13] measurements were taken at a distance of approximately 10 vessel diameters from the aneurysm location so that BCs to the numerical models could be applied at a sufficient distance from the location of the aneurysm. Measurement

Figure 3: A comparison of VFR waveforms from CoA patient (marked-red) measured in proximal ICA and average VFR waveforms from healthy volunteers (marked-blue) in the same location. The flow-rates in presence of CoA are 1.5 times higher (5.44 ml/sec) as compared with the normal healthy individuals (3.62 ml/sec). Solid horizontal lines represent average values of VFR for CoA (red) and typical (blue).
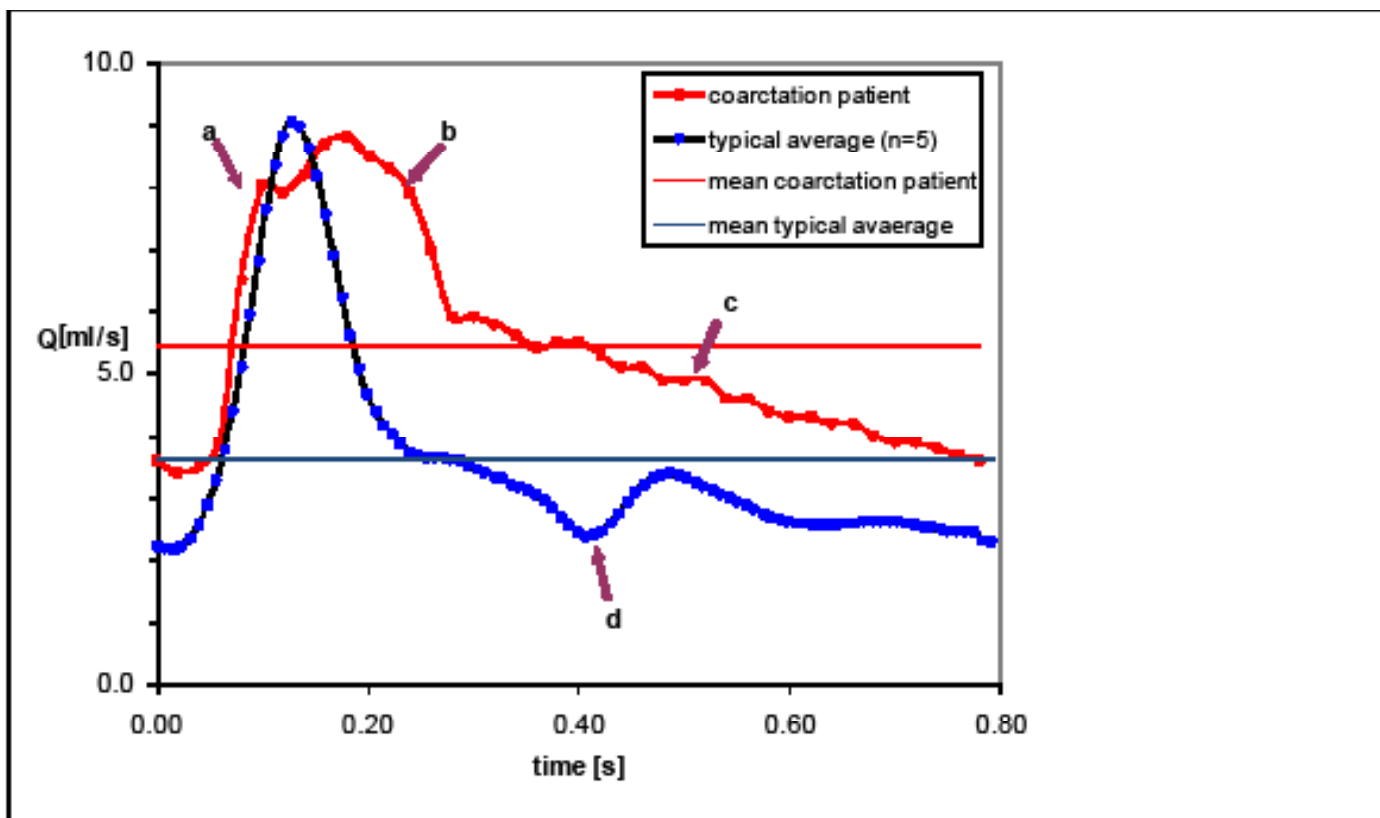
Table-1: Radiological characteristics of the IA included in the study, the pc-MR measurements in CoA patient and healthy volunteers along with the locations, types and methods of BC application

IA Location, Size* and Neck Size*	Q-flow measurements using pc-MR and BC application						
Lt ICA Subclinoid, 1.8mm, 3.1mm	Location of Q-Flow measurements	Q-av-Typical Healthy Volunteers (ml/s)	Q-av-CoA patient (ml/s)	Change (%)	BC location	BC type	BC Method†
	1. Lt ICA Proximal	3.95	5.44	+27.4	1. Lt ICA Proximal	Inlet/velocity	pc-MR
	2. Lt ICA Distal	3.7	5.07	+27.1	2. Lt ICA Distal	Outlet/velocity	pc-MR
	4. Lt ACA	1.2	2.66	+54.9	3. Lt OphthA	Outlet/pressure	Typical/population average

NB: Q-av; average blood flow, BC; boundary condition, Lt; left, Rt; right, ICA; internal carotid artery, MCA; middle cerebral artery, OphthA; ophthalmic artery, *size is reported as max diameter. †BC method refers to the analyses based on patient-specific BC from CoA patient.

location in distal vessels was approximately 3 diameters from the IA.

Measurements are reported in Fig-3 and Table-1. The manufacturer's proprietary post-data-acquisition processing software (Q-Flow™, Philips® Medical Systems, Best, The Netherlands) was used to estimate VFR waveforms at each spatial location.

Transthoracic Doppler echocardiography: Flow and pressure measurements were performed using transthoracic Doppler echocardiography (Philips® Sonos™ 5500). The results are reported in Fig-5.

Numerical 3D models and computational fluid dynamics (CFD) analysis: The @neurIST computational tool-chain was used to reconstruct vessel and aneurysmal geometries, as described by Marzo et al.[66] The 3D transient Navier–Stokes equations were solved by using the finite-control-volume software ANSYS®-CFX™. Blood was assumed to be incompressible, with density ρ=1060 kg/m^3 and Newtonian, with viscosity μ=0.0035 Pa·s. The relevant hemodynamic indices were computed (Table-2) in the IA located in subclinoid part of left ICA (Fig-2) of the patient using the VFR values measured in the patient as BCs. A second analysis was performed with BCs derived from the average VFR values measured in healthy volunteers. Location, type and method of BC applied in the study are indicated in Table-1. All analyses were run in parallel on two Itanium2® 900 MHz 64-bit processors. The average time required to solve one cardiac cycle was approximately 8.6 Hr. Analyses were run for three cardiac cycles, to minimize the effects of the initial transient effects, and only results from the last cardiac cycle were post-processed.

Results

Flow measurements in intracranial arteries of healthy volunteers and patient with CoA

On comparing the patient-specific waveforms (Fig-3) from CoA patient (red) with that of typical normal individual (blue) it becomes apparent that the VFR waveform in the proximal ICA of CoA patient is higher than the one for the healthy volunteers. This is also reflected by the average values reported in Table-1 where the flow-rates for the CoA patient are 1.5 times higher (5.44 ml/sec) as compared to the normal healthy individuals (3.62 ml/sec).

The flow waveforms further illustrate that the cerebral arterial flow in CoA rises and falls slowly than that of a typical individual but the overall volume over one cardiac cycle is increased from 3.48 ml to 4.54 ml. A new broad hump (arrow-b) is seen just after the original peak (arrow-a). The systolic upstroke is delayed and slow; the peak is broader (between arrows a & b), slightly lower and dumped. The flow during diastole is almost a smooth decline curve (arrow-c) and the notch indicating the beginning of diastole is absent (arrow-d).

Contour plots for hemodynamic indices and their absolute values

Figure 4: Time-averaged WSS (top) and OSI (Oscillatory shear index) (bottom) contour plots in the left subclinoid intracranial aneurysm of the CoA patient. Whereas, areas affected by high WSS are increased in CoA patient (top, right) as compared with healthy volunteers (top, left) OSI patterns are minimally changed.
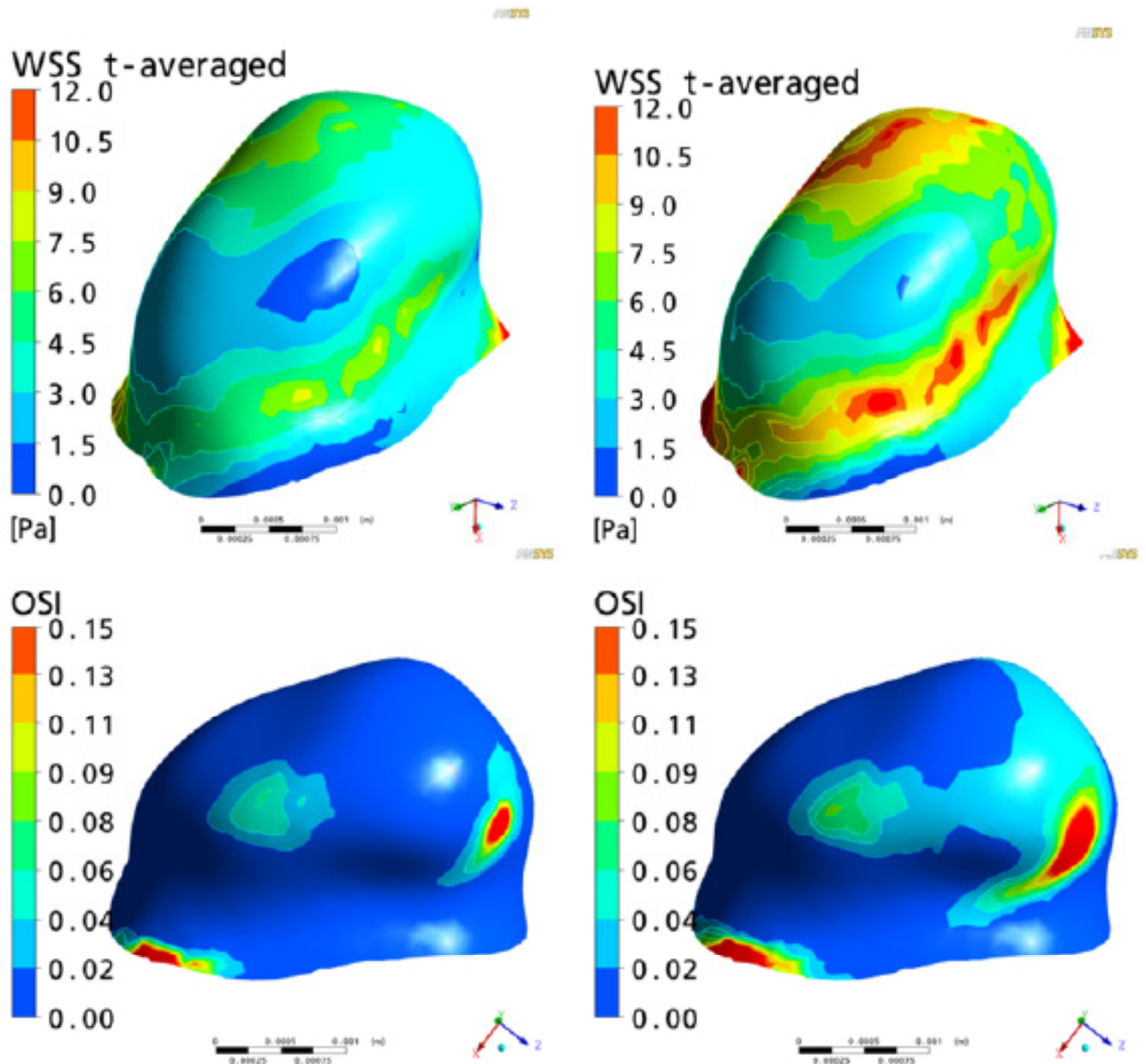
Table 2: Absolute values of WSS, OSI, velocity and pressure for IA, obtained using BCs derived from healthy volunteers and measurements taken in CoA patient by pc-MR

Hemodynamic Indices	BCs derived from healthy volunteers (without CoA)	BCs derived from patient (with CoA)	% difference
Max t-ave velocity (m/s)	0.5	0.72	+44
Space and t-ave velocity (m/s)	0.072	0.097	+35
Max OSI	0.3	0.3	0
Area of WSS below 0.4 Pa (mm2)	0.05 (0.3%)	0.03 (0.2%)	-34
Area of WSS above 15 Pa (mm2)	0.4 (0.4%)	3.0 (17.2%)	+650
Space and t-ave WSS in aneurysm (Pa)	5.7	9.4	+65
Max pressure on aneurysm wall (mmHg)*	122.4	140.8	+15
Area of elevated pressure (mm2)*	3.0 (17.1%)	1.5 (8.5%)	-50%

NB: WSS; wall shear stress, OSI; oscillatory shear index, Max; maximum, ave; average, t; time, BC; boundary condition, * indicates the values at peak systole

Figure 5: Transthoracic Doppler echocardiogram showing aortic coarctation with a diastolic tail. A coarctation gradient of 30-40mmHg was seen (arrowhead) while the average aortic pressure gradient was 16 mmHg. The peak velocity in aorta was 276cm/sec.
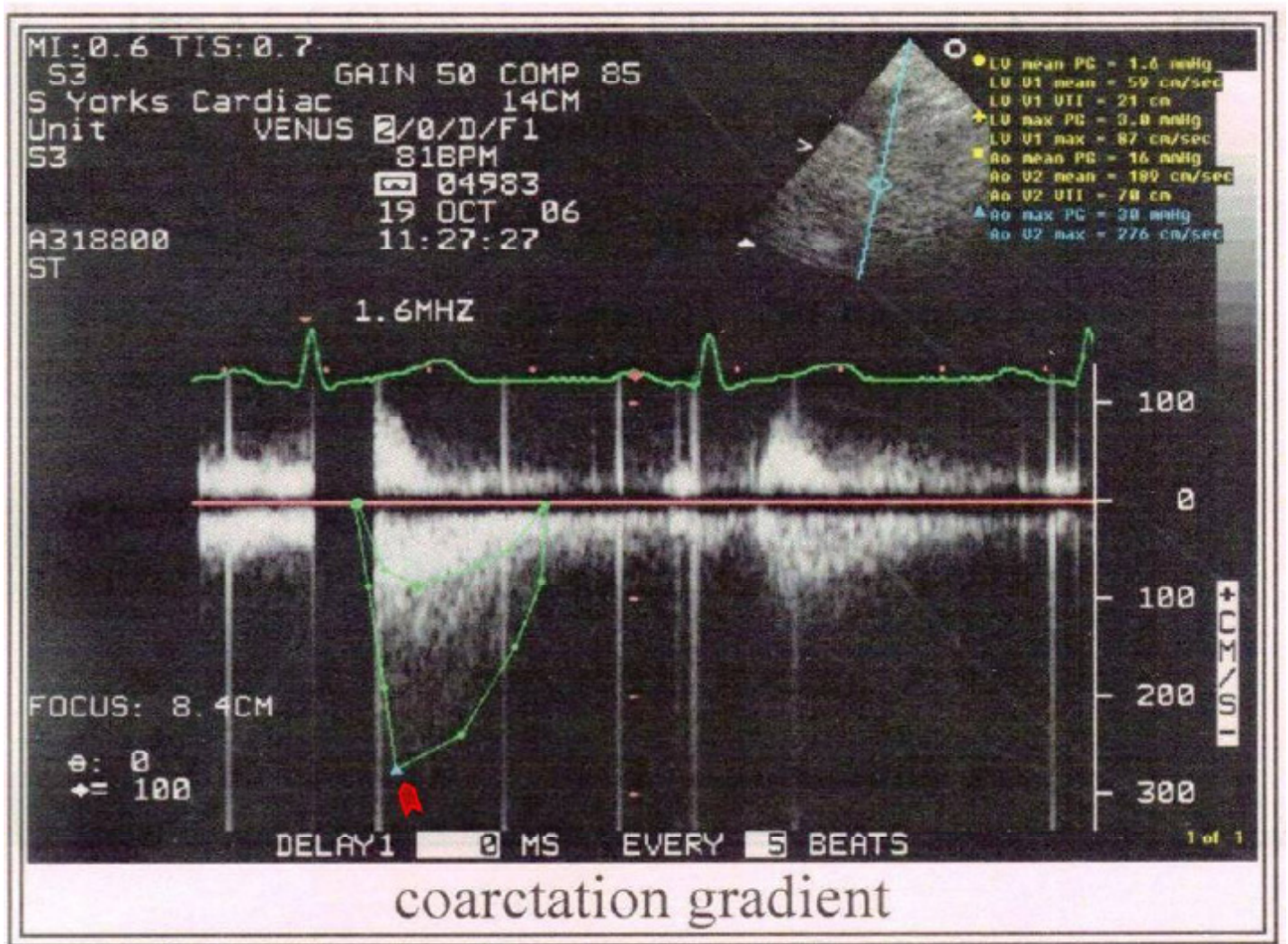
Discussion

The CoA is a connective tissue disorder accounting for 10% of the cases of congenital heart disease.[103] The most common site of narrowing is distal to the left subclavian artery. Due to the mechanical outflow obstruction and extensive collateral formation a number of hemodynamic changes are seen in CoA. The most notable is a differential hypertension produced in the segment of aorta above the site of narrowing leading to increased aorto-cranial pressure gradients[1,36,45,71,102] and dilatation of cervico-cephalic arteries.[1,85] Similar changes were seen in our patient (Fig-5). A pressure gradient of 30-40 mmHg was present at the site of coarctation as compared to the mean aortic pressure gradient of 16 mmHg. The peak velocity in aorta was also increased to 276 cm/sec when compared to the peak velocity of 80-90 cm/sec in the aorta of a normal person.[19] As discussed in the previous sections, it is hypothesized here that the regional cerebral blood flow (rCBF) in CoA patients should increase as a consequence of these changes.

It is surprising to see that such little attention is devoted on the effects of CoA on rCBF. The first available study on the subject was conducted by Hafkenschiel et al[37] in 1949. They measured rCBF and cerebral oxygen consumption in two patients with CoA using nitrous oxide (N_2O) saturation method and found that the rCBF in patients with CoA was higher as compared with normal subjects.

A similar study was done by Rowe and colleagues[85] in 1964 who measured the rCBF in 20 CoA patients using the same technique. The rCBF was measured in these patients before and after the surgical correction of CoA and the results were compared with rCBF values obtained in normal subjects in their previous study,[86] and rCBF values specific to hypertensive patients.[18] No significant differences were noted in the rCBF pre and post surgical repair of coarctation and, between CoA patients and hypertensive patients. Interestingly, the comparison of rCBF in CoA patients and healthy volunteers suggested that the values of average rCBF measured by them (63±13 ml/100 gm/ min) were approximately 21% higher compared to the rCBF measured in 8 normal subjects (52±12 ml/100 gm/ min)[86] but not statistically significant . The postoperative measurements in this study were taken at an average interval of 21 months (maximum 9.25 yrs) from the time of surgery which may have obscured some of the differences. Re-occurrence of coarctation is a frequent complication following surgery that can occur in 41-86% patients.[44] The similar patterns were observed in our patient where 60-70% loss of luminal diameter occurred 14 years after repair. As the diameter of aorta was not assessed by Rowe and colleagues[85] at the time of rCBF measurements, the possibility of recoarctation in these patients cannot be ruled out which might account for the lack of difference in the rCBF before and after surgical correction.

The measurements of rCBF in both studies were performed using the oldest available technique based on N_2O diffusion and Fick's principle introduced by Kety and Schmidt in 1951.[57] The technique provides the measurements of global CBF rather than the regional values. The accuracy of measurements is dependent upon the reliability of the blood sample withdrawn from a single jugular vein which can be influenced by the flow variations in dural sinuses and torcula.[52] With the advent of new technology, the technique of rCBF measurement has evolved tremendously. The use of pc-MR in this context is gaining a rapid popularity.[10,25,26,84,101,107] The rCBF can be measured using this technique in a simple non-invasive manner without the need of any intravenous contrast administration and has been validated widely by means of in vitro and in vivo experiments.[8,12,28,58]

Recent evidence however indicates that the local variations in the hemodynamics that play an important role in the etiopathogenesis of IAs[32,38,40-42,65,69,72,104] highlighting the importance of assessing the local flow patterns. No previous study however has examined the local hemodynamics in presence of CoA. According to the Hagan-Poiseuille law, we hypothesized that the local VFR should increase in patients with CoA. The pc-MR measurements performed prior to repair of the CoA in our study confirmed this hypothesis by demonstrating an increase of local regional CBF by 27.1 to 54.9% (Table-1) in ICA and ACA respectively, when compared to healthy volunteers. As a result space and time averaged velocity and max time average velocities inside the coincidental IA present were also increased by 35-44% (Table-2) when the BCs specific to CoA were used.

We further hypothesize that the increased VFR can be an important contributory factor in the increased incidence of IAs in presence of CoA. The possible mechanisms responsible for increased incidence of IAs in CoA patients are explored in the further sections of this manuscript. Eppinger was the first person to draw attention towards the association between CoA and IAs in 1871.[27] Whereas the exact mechanisms responsible for this increased incidence remained obscure, arterial hypertension has been suggested as a possible underlying cause by most of the authors (Table-3).[3,9,24,50,75,78,92,95] Stehbens was the strongest proponent of this theory who particularly stressed on the importance of hypertension in this context while denying the role of all other factors including vessel wall abnormalities.[92,95] This assumption is probably based on two observations. First, hypertension is often a constant feature in CoA patients. Second, hypertension has been considered as a major risk factor for the development of IAs even without CoA.[22,99] In spite of an increased prevalence of IAs in hypertensive patients the role of hypertension in this context has been questioned by many authors. McCormick and Schmalstieg found no relationship between arterial hypertension and IAs in 250 patients they studied.[67] In a similar study conducted in 212 cases, Andrews and Spiegel[6] did not find significant elevation in the blood pressure in patients with IAs compared with the general population. However, studies supporting hypertension as a risk factor for the development and rupture of IAs outnumber the studies refuting it. De la Monte et al[22] found high degree of correlation (p<0.001) between systemic hypertension and development of saccular IAs. In one of the largest studies conducted including 20,767 elderly patients Taylor et al[99] found hypertension as an independent major risk factor for aneurysmal SAH.

Although, hypertension can be an important contributory

Table-3: A comprehensive review of different mechanisms proposed for the increased incidence of IAs in CoA patients

Author/ Year	No. of Patients	IA location/No.	HTN at the time IA diagnosed	Associated features	Proposed Mechanism(s)
Abbot (1928) [1]	6	ACA, AcomA, VA, PcomA, MCA	Yes	Reported one case of his own (MCA), rest 5 cases collected from literature	Congenital IA
Laitinen et al (1960) [62]	1	Pericallosal/ Callosomarginal	Yes	Oxycephalic deformity of skull	Possible developmental errors
Patel et al (1971) [78]	7	ICA, AcomA(3), ACA(3), PcomA, BA	Yes	Only pediatric population (<19 yrs) reviewed, 12% had CoA coexisting with IAs	HTN
Banna et al (1971) [9]	1	PCA	NA	Source of SAH was dilated spinal collaterals	Medial hypoplasia of arteries of CoW + HTN
Stehbens (1989) [92]				Review article	HTN
Orsi et al. (1993) [75]	1	MCA, ICA	NA	-	HTN
Schievink et al (1996)[87]	1	MCA	No	-	Development errors of Neural Crest leading to defective collagen and elastin formation
Ishii et al (2001) [50]	1	AcomA	Yes	Coarctation of abdominal aorta	HTN
Ahmetoglu et al (2002) [3]	1	B/L MCA	Yes	Coarctation of abdominal aorta	HTN ± hemodynamic shear stress
Mercado et al. (2002)[70]	3	ICA, PcomA(2), PeriA	Yes	Provided a comprehensive review of the distinct clinical behavior of IAs in presence of CoA	Development errors of Neural Crest
Connolley et al (2003)[15]	10	ICA, MCA, PICA, PCA, PcomA, AChoA, BA tip	Yes (in 7 out of 10 patients)	Found 10% incidence of IAs in patients with CoA, no significant difference in BP of patients with and without IAs	Development errors of Neural Crest
Cowan et al (2004)[17]	1	PcomA	No	Coexisting Alagille syndrome (arteriohepatic dysplasia), progression of infundibulum to PcomA Aneurysm	Developmental defects
Harikrishnan (2005) [39]	1	BA, VA	Yes	CoA of Descending aorta, coronary artery aneurysms	Atherosclerosis
Hudaoglu et al (2006)[48]	1	PcomA	No	Raised strong suspicions about HTN alone being a factor for the increased incidence of IA in CoA	Development errors of Neural Crest
Kan et al (2007) [53]	1	ICA	NA	Fusiform aneurysm associated with PHACES syndrome, positive family history of IAs	Development errors of Neural Crest
Singh et al (2009) (Present study)	1	ICA, MCA, PeriA	No	Measured the CBF in CoA patient and proposed WSS as an important factor in the formation of IAs in these patients	Hemodynamic WSS

NB: PHACES syndrome; posterior fossa malformations, facial hemangiomas, arterial anomalies, CoA, cardiac defects, eye abnormalities and sterna defects, NA; not available, B/L; bilateral, CoW; circle of Willis, BP; blood pressure, PeriA; pericallosal artery, AChoA; anterior choroidal artery, PCA; posterior cerebral artery, BA; basilar artery, VA; vertebral artery, PICA; posterior inferior cerebeller artery, HTN; Hypertension, MCA,ICA & ACA; middle, internal & anterior cerebral arteries.

force in the etiopathogenesis of IAs in these patients, it cannot be the sole contributor. Hudaoglu et al[48] raised a question on hypertension alone being a factor in the etiopathogenesis of IAs in CoA patients. The fact is further supported by the observation that IAs may develop or rupture even in normotensive patients, years after the repair of CoA.[30,61,70,76] Additionally, hypertension was not uniformly noted in the patients of CoA reported to have IAs.[15,87] The IAs were developed in our patient 17 years after the surgical correction of CoA. However, recoarctation of the repaired segment occurred during this period (>70% reduction in aortic diameter), the patient remained completely asymptomatic with a very well controlled blood pressure (Fig-1). Our findings also indicate towards the role of other factors working independent of arterial hypertension.

Laitinen and Snellman[62] in 1960 found that apart from CoA, aneurysms of Pericallosal artery region were also associated with other concomitant malformations such as craniosynostosis and kyphoscoliosis. They believed that coexistence of these malformations with IAs is secondary to a common developmental error playing a role in their etiology. Embryologically; heart, aorta and cervico-cephalic arteries all share a common origin from neural crest. After recognizing the association between a variety of congenital heart diseases and IAs, Schievink et al[87] attributed the occurrence of IAs in CoA patients to the developmental errors of neural crest resulting in abnormal vessel wall collagen. The same theory was later supported many other authors (Table-3).[15,17,48,53,70]

Hemodynamic stress due to increased blood flow has long been implicated in the pathogenesis of IAs. Development of IAs is reported in association with a wide range of conditions responsible for increased flow related WSS. Padget was first to draw attention towards the relationship between anatomical variations in circle of Willis and increased incidence of IAs.[77] The similar findings were confirmed by other workers.[4,82,94] Kayambe et al[56] observed that there was a definitive correlation between the site of vascular asymmetry and the location of IA formation. This increased incidence of IAs in presence of vascular asymmetry is thought to be caused by increased hemodynamic stress secondary to compensatory increase in blood flow.[56,93,94]

Iatrogenic carotid artery ligation is a well established technique to produce IAs in experimental animals.[38,40-42,51,73] Increased hemodynamic shear stress has been considered a major factor in the production of these experimental IAs.[32,38,40-42,51,73] Apart from the carotid ligation, induced hypertension and administration of BAPN (beta aminopionitrile; a lathyrogen used to render arterial walls fragile), can potentiate the occurrence of IAs in these models . Handa et al[38] divided their experimental animals into three cohorts: no carotid ligation, unilateral carotid ligation and bilateral carotid ligation. Whereas, all rats were made hypertensive and fed on BAPN, no IA was induced where carotid artery was not ligated. Furthermore, the IAs was always formed corresponding to the sites where hemodynamic stress was expected to increase after carotid ligation.

Congenital absence of ICA,[14,47,96] arterivenous malformations (AVMs),[68,81,100] Takayasu's arteritis,[54,98] Moyamoya disease,[2,55,59] and presence of persistent fetal circulation[5,63,109] are other similar conditions where increased IAs are encountered due to increased-flow-related WSS. Development of IAs has also been observed following extra-intracranial bypass procedures,[29,60,74] again secondary to increased rCBF. Resolution of these flow related IAs can occur once the cerebral hemodynamics is reestablished by addressing the underlying pathology.[79,97]

The importance of hemodynamic WSS in the context of CoA is somewhat poorly explored. Ahmetoglu et al (2002)[3] indicated that arterial wall injury secondary to increased hemodynamic shear forces may be an important factor in the IA formation while discussing their case of abdominal aortic coarctation (AbCoA). However, the statement probably reflects their opinion towards the etiopathogenesis of IAs in general population rather than in patients with CoA. Furthermore, the inference was merely based on the literature based evidence rather than any experimental work. They finally concluded that hypertension was the main factor responsible for the rupture and growth of IAs in patients with AbCoA.[3]

We hypothesize that the higher WSS values secondary to increased flow-rates in cerebral circulation can be an important contributory factor in the pathogenesis of IAs in presence of CoA. WSS is a frictional force exerted tangentially on the arterial endothelium by flowing blood. It is proportional to the blood viscosity and velocity gradients. The average physiological range of arterial WSS has been suggested to lie between 1.5-2.0 Pa by Malek et al.[64] It is widely accepted now that damage to the arterial and subsequently aneurysmal wall by hemodynamic forces plays a crucial role in the etiopathogenesis of IAs.[11,32,38,40-42,65,69,72,91,104] High supra-physiological and low infra-physiological values of WSS have been associated with initiation, growth and rupture of aneurysms.[11,32,38,40-42,65,69,72,91,104] The values of space and time averaged WSS as well as the area affected by supra-physiological WSS (>15Pa) were increased in our patient by 65% and 650%, respectively (Table-2). This exponential rise in the high supra-physiological WSS may play an important role in the etiopathogenesis of IAs in patients with CoA.

Various authors tried to explain the underlying mechanisms involved in the WSS induced vascular remodeling. The normal endothelial cell (EC) function and structure are regulated by WSS through a process called mechanotransduction.[21,20] The shear stress is sensed by a number of mechanoceptors including basal adhesion points of ECs, cell junctions, and nuclear membrane.[21,20] WSS also activates stretch-sensitive ion channels such as phospholipids and integrins in cellular membrane.[21,20] Increased production of matrix metalloproteinase (MMP-13) by ECs has been demonstrated after their prolonged exposure to high WSS which, in turn, leads to degeneration of the internal elastic lamina.[90] It has been demonstrated by a number of workers[16,31,80] that WSS increases endothelial production of nitric oxide (NO) by inducing an enzyme responsible for its synthesis (iNOS; inducible nitric oxide synthase). Fukuda et al[31] found a high concentration of iNOS at the site of IA formation, in both rat and human arteries and concluded that iNOS is a prerequisite for

de novo development of IAs in cerebral vessels. In 1995, Wang et al[104] showed that smooth muscle cells (SMCs) in arterial wall can also respond to WSS in intact arteries by virtue of interstitial flow generated by transmural flow gradients, further accentuating the vessel wall damage.

In addition to WSS, oscillatory shear index (OSI) has also been recognized as an important hemodynamic factor in the aneurysmal pathogenesis.[33-35,43,65] It is a measure of the oscillatory nature of shear forces.[33-35,43,65] This index, which has a range of between 0 and 0.5, represents the fraction of the cardiac cycle over which the instantaneous shear force vector forms an angle greater than 90 degrees to the time-average direction of the same force. Consistently high values of OSI have been associated with EC dysfunction.[43] Changes in cell structure secondary to cyclic mechanical stress have been demonstrated by Wang et al.[104] resulting in disruption of the actin cytoskeleton of ECs. Glor and colleagues propose 0.2 as a threshold value for OSI above which endothelial damage is initiated.[33,34] Whereas, no change was observed in the maximum OSI in presence of CoA (Table-2), the values obtained from both analyses (0.3) remained above this critical threshold. This indicates towards the possible role of high OSI in the EC damage in patients with IAs irrespective of presence or absence of CoA.

Apart from being a known risk factor for the formation of IAs, CoA has also been associated with increased incidence of IA rupture (4.8%).[15,48,70,106] No satisfactory explanation is provided for the association between the two entities. This increased tendency for early aneurysmal rupture can possibly be explained by analyzing the hemodynamic factors computed for our patient (Table-2). Whereas the values for maximum pressure on IA wall have increased by 15% in patient with CoA, the area affected by high pressure is actually decreased by 50%. In other words, in the context of our CoA patient, the pressure on the IA wall is more focal in nature in presence of CoA and may be an important underlying factor predisposing to early aneurysmal rupture. High supra-physiological values of WSS have also been associated with endothelial cell dysfunction.[11,32,38,40-42,64,65,69,72,91,104] The exponential rise (by 650%) in the area affected by high supra-physiological WSS (>15Pa) may also play a role in early IA rupture in patient with CoA.

Limitations of the study

Due to technical limitations, we could not perform extensive measurements in cerebral arteries other than ICA and ACA. It is however expected that the VFR will increase in other arteries as well provided other parameters in the Hagan-Poiseuille (Eq-1) equation remain constant. The current study therefore reflects the need of further studies performed in larger cohort of patients with CoA.

Conclusions

Our study demonstrates that the cerebral arterial flow-rates in CoA patients are significantly higher when compared with average arterial flow-rates in healthy population. Furthermore,

the values of space and time averaged WSS and the area affected by supraphysiological WSS (>15Pa) were increased in our patient by 65% and 650%, respectively. The values of maximum OSI however, remained unaffected by the presence of CoA. Increased hemodynamic WSS secondary to the increased rCBF may play an important role in the pathogenesis of IAs in CoA patients. The more focalized pressure impingement on the aneurysmal wall in CoA patients may be an important underlying factor affecting the early aneurysmal rupture.

The lack of clear knowledge about the rCBF in CoA patients and the existing controversies in the etiopathogenesis of IAs in these patients emphasizes the importance of the findings of the current study.

Acknowledgements

Ethical Approvals

The project has appropriate ethical approvals for the required research. The ethical matters are managed by Project Ethical Committee, Oxford, UK (Oxfordshire Research Ethics Committee-A Study Number: 07/Q1604/53). A copy of the ethical approval can be provided as and when required.

References:

1. Abbott ME. A statistical study and historical retrospect of 200 recorded cases, with autopsy, of stenosis or obliteration of the descending arch in subjects above the age of two years. Am Heart J:1928;392-421.

2. Adams HP, Jr., Kassell NF, Wisoff HS, Drake CG. Intracranial saccular aneurysm and moyamoya disease. Stroke 10:1979;174-179.

3. Ahmetoğlu A, Koşucu P, Sari A, Gümele HR. Abdominal aortic coarctation associated with multiple intracranial aneurysms. European Journal of Radiology Extra (46):2003;38-41.

4. Alpers BJ, Berry RG. Circle of Willis in cerebral vascular disorders. The anatomical structure. Arch Neurol 8:1963;398-402.

5. Ali S, Walker MT. Bilateral persistent trigeminal arteries associated with bilateral carotid aneurysms. J Vasc Interv Radiol. 2007;18:692-694.

6. Andrews RJ, Spiegel PK. Intracranial aneurysms. Age, sex, blood pressure, and multiplicity in an unselected series of patients. J Neurosurg. 1979;51:27-32.

7. Atkinson JL, Sundt TMJ, Houser OW, Whisnant JP. Angiographic frequency of anterior circulation intracranial aneurysms. J Neurosurg. 1989;70:551-555.

8. Bakker CJ, Kouwenhoven M, Hartkamp MJ, Hoogeveen RM, Mali WP. Accuracy and precision of time-averaged flow as measured by nontriggered 2D phase-contrast MR angiography, a phantom evaluation. Magn Reson Imaging. 1995;13:959-965.

9. Banna MM, Rose PG, Pearce GW. Coarctation of the aorta as a cause of spinal subarachnoid hemorrhage. Case report. J Neurosurg. 1973;39:761-

763.

10. Buijs PC, Krabbe-Hartkamp MJ, Bakker CJ, et. al. Effect of age on cerebral blood flow: measurement with ungated two-dimensional phase-contrast MR angiography in 250 adults. Radiology. 1998;209:667-674.

11. Burleson AC, Strother CM, Turitto VT. Computer modeling of intracranial saccular and lateral aneurysms for the study of their hemodynamics. Neurosurgery. 1995;37:774-82; discussion 782-7782; discussion 782-4.

12. Caputo GR, Kondo C, Masui T, et. al. Right and left lung perfusion: in vitro and in vivo validation with oblique-angle, velocity-encoded cine MR imaging. Radiology. 1991;180:693-698.

13. Castro MA, Putman CM, Cebral JR. Computational fluid dynamics modeling of intracranial aneurysms: effects of parent artery segmentation on intra-aneurysmal hemodynamics. AJNR Am J Neuroradiol. 2006;27:1703-1709.

14. Chen L, Liu J-M, Zhou D. Congenital absence of the right common carotid artery, internal carotid artery and external carotid artery associated with anterior communicating artery aneurysm: a rare case. Neurol Sci. 2008;29:485-487.

15. Connolly HM, Huston J3rd, Brown RDJ, et. al. Intracranial aneurysms in patients with coarctation of the aorta: a prospective magnetic resonance angiographic study of 100 patients. Mayo Clin Proc. 2003;78:1491-1499.

16. Cooke JP, Stamler J, Andon N, et. al. Flow stimulates endothelial cells to release a nitrovasodilator that is potentiated by reduced thiol. Am J Physiol. 1990;259:H804-12.

17. Cowan JAJ, Barkhoudarian G, Yang LJS, Thompson BG. Progression of a posterior communicating artery infundibulum into an aneurysm in a patient with Alagille syndrome. Case report. J Neurosurg. 2004;101:694-696.

18. Crumpton CW, Rowe GG, Capps RC, Whitmore JJ, Murphy QR. The effect of hexamethonium upon cerebral blood flow and metabolism in patients with premalignant and malignant hypertension. Circulation. 1955;11:106-109.

19. Daley PJ, Sagar KB, Wann LS. Doppler echocardiographic measurement of flow velocity in the ascending aorta during supine and upright exercise. Br Heart J. 1985;54:562-567.

20. Davies PF. Flow-mediated endothelial mechanotransduction. Physiol Rev. 1995;75:519-560.

21. Davies PF, Tripathi SC. Mechanical stress mechanisms and the cell. An endothelial paradigm. Circ Res. 1993;72:239-245.

22. de la Monte SM, Moore GW, Monk MA, Hutchins GM. Risk factors for the development and rupture of intracranial berry aneurysms. Am J Med. 1985;78:957-964.

23. Drake CG. Progress in cerebrovascular disease. Management of cerebral aneurysm. Stroke. 1981;12:273-283.

24. Du Boulay GH. Some observations on the natural history of intracranial aneurysms. Br J Radiol. 1965;38:721-757.

25. Enzmann DR, Marks MP, Pelc NJ. Comparison of cerebral artery blood flow measurements with gated cine and ungated phase-contrast techniques. J Magn Reson Imaging. 1993;3:705-712.

26. Enzmann DR, Ross MR, Marks MP, Pelc NJ. Blood flow in major cerebral arteries measured by phase-contrast cine MR. AJNR Am J Neuroradiol. 1994;15:123-129

27. Eppinger H. Stenosis aortae congenita seu isthmus persistans. Vjschr Prakt aheilk. 1871;112:31-67.

28. Evans AJ, Iwai F, Grist TA, et. al. Magnetic resonance imaging of blood flow with a phase subtraction technique. In vitro and in vivo validation. Invest Radiol. 1993;28:109-115.

29. Fleischer AS, Faria MAJ, Hoffmann JCJ. Pseudoaneurysm complicating superficial temporal artery--middle cerebral artery bypass. Surg Neurol. 1979;12:305-306.

30. Forfang K, Rostad H, Sorland S, Levorstad K. Late sudden death after surgical correction of coarctation of the aorta. Importance of aneurysm of the ascending aorta. Acta Med Scand. 1979;206:375-379.

31. Fukuda S, Hashimoto N, Naritomi H, et. al. Prevention of rat cerebral aneurysm formation by inhibition of nitric oxide synthase. Circulation. 2000;101:2532-2538.

32. Gao L, Hoi Y, Swartz DD, et. al. Nascent aneurysm formation at the basilar terminus induced by hemodynamics. Stroke. 2008;39:2085-2090.

33. Glor FP, Ariff B, Hughes AD, et. al. The integration of medical imaging and computational fluid dynamics for measuring wall shear stress in carotid arteries. Conf Proc IEEE Eng Med Biol Soc. 2004;2:1415-1418.

34. Glor FP, Long Q, Hughes AD, et. al. Reproducibility study of magnetic resonance image-based computational fluid dynamics prediction of carotid bifurcation flow. Ann Biomed Eng. 2003;31:142-151.

35. Goubergrits L, Kertzscher U, Schoneberg B, et. al. CFD analysis in an anatomically realistic coronary artery model based on non-invasive 3D imaging: comparison of magnetic resonance imaging with computed tomography. Int J Cardiovasc Imaging. 2008;24:411-421.

36. Gupta TC, Wiggers CJ. Basic hemodynamic changes produced by aortic coarctation of different degrees. Circulation. 1951;3:17-31.

37. Hafkenschiel JHJ, Crumpton CW, Moyer JH. Blood flow and oxygen consumption of the brain in coarctation of the aorta. Proc Soc Exp Biol Med. 1949;71:165-167.

38. Handa H, Hashimoto N, Nagata I, Hazama F. Saccular cerebral aneurysms in rats: a newly developed animal model of the disease. Stroke. 1983;14:857-866.

39. Harikrishnan S, Stigimon J, Tharakan JM. Intracranial aneurysms, coronary aneurysms and descending aortic coarctation--unreported association. Int J Cardiol. 2005;99:329-330.

40. Hashimoto N, Handa H, Hazama F. Experimentally induced cerebral aneurysms in rats. Surg Neurol. 1978;10:3-8.

41. Hashimoto N, Handa H, Nagata I, Hazama F. Experimentally induced cerebral aneurysms in rats: Part V. Relation of hemodynamics in the circle of Willis to formation of aneurysms. Surg Neurol. 1980;13:41-45.

42. Hashimoto N, Kim C, Kikuchi H, et. al. Experimental induction of cerebral aneurysms in monkeys. J Neurosurg. 1987;67:903-905.

43. He X, Ku DN. Pulsatile flow in the human left coronary artery bifurcation: average conditions. J Biomech Eng. 1996;118:74-82.

44. Hesslein PS, McNamara DG, Morriss MJ, Hallman GL, Cooley DA. Comparison of resection versus patch aortoplasty for repair of coarctation in infants and children. Circulation. 1981;64:164-168.

45. Hom JJ, Ordovas K, Reddy GP. Velocity-encoded cine MR imaging in aortic coarctation: functional assessment of hemodynamic events. Radiographics. 2008;28:407-416.

46. Hop JW, Rinkel GJ, Algra A, van Gijn J. Case-fatality rates and functional outcome after subarachnoid hemorrhage: a systematic review. Stroke. 1997;28:660-664.

47. Horie N, Tsutsumi K, Kaminogo M, et. al. Agenesis of the internal carotid artery with transcavernous anastomosis presenting with an anterior communicating artery aneurysm--a case report and review of the literature. Clin Neurol Neurosurg. 2008;110:622-626.

48. Hudaoglu O, Kurul S, Cakmakci H, et. al. Aorta coarctation presenting with intracranial aneurysm rupture. J Paediatr Child Health. 2006;42:477-479.

49. Inagawa T. Trends in incidence and case fatality rates of aneurysmal subarachnoid hemorrhage in Izumo City, Japan, between 1980-1989 and 1990-1998. Stroke. 2001;32:1499-1507.

50. Ishii K, Isono M, Kasai N, et. al. Midaortic syndrome in childhood associated with a ruptured cerebral aneurysm: a case report. Surg Neurol. 2001;55:209-212.

51. Jamous MA, Nagahiro S, Kitazato KT, et. al. Endothelial injury and inflammatory response induced by hemodynamic changes preceding intracranial aneurysm formation: experimental study in rats. J Neurosurg. 2007;107:405-411.

52. Joseph M, Nates, JL. Stable Xenon Computed Tomography Cerebral Blood Flow Measurement In Neurological Disease: Review And Protocols. The Internet Journal of Emergency and Intensive Care Medicine. 2000;4(2).

53. Kan P, Liu JK, Couldwell WT. Giant fusiform aneurysm in an adolescent with PHACES syndrome treated with a high-flow external carotid artery-M3 bypass. Case report and review of the literature. J Neurosurg. 2007;106:495-500.

54. Kanda M, Shinoda S, Masuzawa T. Ruptured vertebral artery-posterior inferior cerebellar artery aneurysm associated with pulseless disease--case report. Neurol Med Chir (Tokyo). 2004;44:363-367.

55. Kawaguchi S, Sakaki T, Morimoto T, Kakizaki T, Kamada K. Characteristics of intracranial aneurysms associated with moyamoya disease. A review of 111 cases. Acta Neurochir (Wien). 1996;138:1287-1294.

56. Kayembe KN, Sasahara M, Hazama F. Cerebral aneurysms and variations in the circle of Willis. Stroke. 1984;15:846-850.

57. Kety SS. The theory and applications of the exchange of inert gas at the lungs and tissues. Pharmacol Rev. 1951;3:1-41.

58. Kondo C, Caputo GR, Semelka R, et. al. Right and left ventricular stroke volume measurements with velocity-encoded cine MR imaging: in vitro and in vivo validation. AJR Am J Roentgenol. 1991;157:9-16.

59. Konishi Y, Kadowaki C, Hara M, Takeuchi K. Aneurysms associated with moyamoya disease. Neurosurgery. 1985;16:484-491.

60. Kurokawa T, Harada K, Ishihara H, et. al. De novo aneurysm formation on middle cerebral artery branches adjacent to the anastomotic site of superficial temporal artery-middle cerebral artery bypass surgery in two patients: technical case report. Neurosurgery. 2007;61:E297-8; discussion E298.

61. Laborde F, Bical O, Lemoine G, Neveux JY. [Rupture of a dissecting aneurysm of the ascending aorta 10 years after therapy of coarctation. Apropos of a case of a 10-year-old girl]. Sem Hop. 1983;59:2937-2938.

62. Laitinen L, Snellman A. Aneurysms of the pericallosal artery: a study of 14 cases verified angiographically and treated mainly by direct surgical attack. J Neurosurg. 1960;17:447-458.

63. Li MH, Li WB, Pan YP, Fang C, Wang W. Persistent primitive trigeminal artery associated with aneurysm: report of two cases and review of the literature. Acta Radiol. 2004;45:664-668.

64. Malek AM, Alper SL, Izumo S. Hemodynamic shear stress and its role in atherosclerosis. JAMA. 1999;282:2035-2042.

65. Mantha A, Karmonik C, Benndorf G, Strother C, Metcalfe R. Hemodynamics in a cerebral artery before and after the formation of an aneurysm. AJNR Am J Neuroradiol. 2006;27:1113-1118.

66. Marzo A, Singh P, Reymond P, et. al. Influence of inlet boundary conditions on the local haemodynamics of intracranial aneurysms. Comput Methods Biomech Biomed Engin. 2009;12:431-444.

67. McCormick WF, Schmalstieg EJ. The relationship of arterial hypertension to intracranial aneurysms. Arch Neurol. 1977;34:285-287.

68. Meisel HJ, Mansmann U, Alvarez H, et. al. Cerebral arteriovenous malformations and associated aneurysms: analysis of 305 cases from a series of 662 patients. Neurosurgery. 2000;46:793-800; discussion 800-800; discussion 800-2.

69. Meng H, Wang Z, Hoi Y, et. al. Complex hemodynamics at the apex of an arterial bifurcation induces vascular remodeling resembling cerebral aneurysm initiation. Stroke. 2007;38:1924-1931.

70. Mercado R, Lopez S, Cantu C, et. al. Intracranial aneurysms associated with unsuspected aortic coarctation. J Neurosurg. 2002;97:1221-1225.

71. Mohiaddin RH, Kilner PJ, Rees S, Longmore DB. Magnetic resonance volume flow and jet velocity mapping in aortic coarctation. J Am Coll Cardiol. 1993;22:1515-1521.

72. Morimoto M, Miyamoto S, Mizoguchi A, et. al. Mouse model of cerebral aneurysm: experimental induction by renal hypertension and local hemodynamic changes. Stroke. 2002;33:1911-1915.

73. Nagata I, Handa H, Hashimoto N, Hazama F. Experimentally induced cerebral aneurysms in rats: Part VI. Hypertension. Surg Neurol. 1980;14:477-479.

74. Nishimoto T, Yuki K, Sasaki T, et. al. A ruptured middle cerebral artery aneurysm originating from the site of anastomosis 20 years after extracranial-intracranial bypass for moyamoya disease: case report. Surg Neurol. 2005;64:261-5; discussion 265.

75. Orsi P, Rosa G, Liberatori G, Lunardi PP, Ferrante L. Repair of two unruptured intracranial aneurysms in the presence of coarctation of the aorta-anesthetic implications and management. J Neurosurg Anesthesiol. 1993;5:48-51.

76. Ostergaard JR, Hog E. Incidence of multiple intracranial aneurysms. Influence of arterial hypertension and gender. J Neurosurg. 1985;63:49-55.

77. Padget DH. The circle of Willis: its embryology and anatomy. In: Dandy WE, ed. Intracranial Arterial Aneurysms. New York, NY: Comstock Publishing Co; 1944:67-90.

78. Patel AN, Richardson AE. Ruptured intracranial aneurysms in the first two decades of life. A study of 58 patients. J Neurosurg. 1971;35:571-576.

79. Peltier J, Vinchon M, Soto-Ares G, Dhellemmes P. Disappearance of a middle cerebral artery aneurysm associated with Moyamoya syndrome after revascularization in a child: case report. Childs Nerv Syst. 2008;24:1483-1487.

80. Pohl U, Herlan K, Huang A, Bassenge E. EDRF-mediated shear-induced dilation opposes myogenic vasoconstriction in small rabbit arteries. Am J Physiol. 1991;261:H2016-23.

81. Redekop G, TerBrugge K, Montanera W, Willinsky R. Arterial aneurysms associated with cerebral arteriovenous malformations: classification, incidence, and risk of hemorrhage. J Neurosurg. 1998;89:539-546.

82. Riggs HE, Rupp C: Miliary aneurysms: Relations of anomalies of circle of Willis to formation of aneurysms. Arch Neurol Psychiat 49:1943;615-616.

83. Reifenstein GH, Levine SA, Gross RE. Coarctation of the aorta. A review of 104 autopsied cases of the "adult type", 2 years of age or older. Am Heart J 1947; 33(2): 146-169.

84. Rordorf G, Koroshetz WJ, Copen WA, et. al. Diffusion – and perfusion-weighted imaging in vasospasm after subarachnoid hemorrhage. Stroke. 1999;30:599-605.

85. Rowe GG, Castillo CA, Afonso S, Young WP, Crumpton CW. Cerebral blood flow in coarctation of the aorta. J Clin Invest. 1964;43:1922-1927.

86. Rowe GG, Maxwell GM, Castillo CA, Freeman DJ, Crumpton CW. A study in man of cerebral blood flow and cerebral glucose, lactate and

pyruvate metabolism before and after eating. J Clin Invest. 1959;38:2154-2158.

87. Schievink WI, Mokri B, Piepgras DG, Gittenberger-de Groot AC. Intracranial aneurysms and cervicocephalic arterial dissections associated with congenital heart disease. Neurosurgery. 1996;39:685-9; discussion 689-69; discussion 689-90.

88. Sekhar LN, Heros RC. Origin, growth, and rupture of saccular aneurysms: a review. Neurosurgery. 1981;8:248-260.

89. Shearer WT, Rutman JY, Weinberg WA, Goldring D. Coarctation of the aorta and cerebrovascular accident: a proposal for early corrective surgery. J Pediatr. 1970;77:1004-1009.

90. Sho E, Sho M, Singh TM, et. al. Arterial enlargement in response to high flow requires early expression of matrix metalloproteinases to degrade extracellular matrix. Exp Mol Pathol. 2002;73:142-153.

91. Singh PK, Marzo A, Coley SC, et. al. The role of computational fluid dynamics in the management of unruptured intracranial aneurysms: a clinicians' view. Comput Intell Neurosci. 2009:760364.

92. Stehbens WE. Etiology of intracranial berry aneurysms. J Neurosurg. 1989;70:823-831.

93. Stehbens WE. Pathology of the Cerebral Blood Vessels. St Louis, Mo: CV Mosby; 1972.

94. Stehbens WE. Aneurysms and anatomical variation of cerebral arteries. Arch Pathol. 1963;75:45-64.

95. Stehbens WE. Cerebral aneurysms and congenital abnormalities. Australas Ann Med. 1962;11:102-112.

96. Suyama K, Mizota S, Minagawa T, et. al. A ruptured anterior communicating artery aneurysm associated with internal carotid artery agenesis and a middle cerebral artery anomaly. J Clin Neurosci. 2009;16:585-586.

97. Takahashi M, Fujimoto T, Suzuki R, et. al. [A case of spontaneous middle cerebral artery occlusion associated with a cerebral aneurysm angiographically disappearing after STA-MCA anastomosis]. No Shinkei Geka. 1997;25:727-732.

98. Takayama K, Nakagawa H, Iwasaki S, et. al. Multiple cerebral aneurysms associated with Takayasu arteritis successfully treated with coil embolization. Radiat Med. 2008;26:33-38.

99. Taylor CL, Yuan Z, Selman WR, Ratcheson RA, Rimm AA. Cerebral arterial aneurysm formation and rupture in 20,767 elderly patients: hypertension and other risk factors. J Neurosurg. 1995;83:812-819.

100. Thompson RC, Steinberg GK, Levy RP, Marks MP. The management of patients with arteriovenous malformations and associated intracranial aneurysms. Neurosurgery. 1998;43:202-11; discussion 211-2011; discussion 211-2.

101. Ueda T, Yuh WT, Taoka T. Clinical application of perfusion and diffusion MR imaging in acute ischemic stroke. J Magn Reson Imaging. 1999;10:305-309.

102. Varaprasathan GA, Araoz PA, Higgins CB, Reddy GP. Quantification of flow dynamics in congenital heart disease: applications of velocity-encoded cine MR imaging. Radiographics. 2002;22:895-905; discussion 905-905; discussion 905-6.

103. Verheugt CL, Uiterwaal CSPM, Grobbee DE, Mulder BJM. Long-term prognosis of congenital heart defects: a systematic review. Int J Cardiol. 2008;131:25-32.

104. Wang DM, Tarbell JM. Modeling interstitial flow in an artery wall allows estimation of wall shear stress on smooth muscle cells. J Biomech Eng. 1995;117:358-363.

105. Wang Z, Kolega J, Hoi Y, et. al. Molecular alterations associated with aneurysmal remodeling are localized in the high hemodynamic stress region of a created carotid bifurcation. Neurosurgery. 2009;65:169-77; discussion 177-1677; discussion 177-8.

106. Weir B, Macdonald, RL: Intracranial aneurysms and subarachnoid hemorrhage: an overview, in Wilkins RH, Rengachary SS (ed): Neurosurgery, ed 2. New York: McGraw-Hill;1996:2191–2213.

107. Yamashita S, Isoda H, Hirano M, et. al. Visualization of hemodynamics in intracranial arteries using time-resolved three-dimensional phase-contrast MRI. J Magn Reson Imaging. 2007;25:473-478.

108. Yong-Zhong G, van Alphen HA. Pathogenesis and histopathology of saccular aneurysms: review of the literature. Neurol Res. 1990;12:249-255.

109. Zada G, Breault J, Liu CY, et. al. Internal carotid artery aneurysms occurring at the origin of fetal variant posterior cerebral arteries: surgical and endovascular experience. Neurosurgery. 2008;63:ONS55-61; discussion ONS61-61; discussion ONS61-2.